scientific reports

Check for updates

OPEN

Spin structures of the ground states of four body bound systems with spin 3 cold atoms

Y. M. Liu[1] & C. G. Bao[2]✉

We consider the case that four spin-3 atoms are confined in an optical trap. The temperature is so low that the spatial degrees of freedom have been frozen. Exact numerical and analytical solutions for the spin-states have been both obtained. Two kinds of phase-diagrams for the ground states (g.s.) have been plotted. In general, the eigen-states with the total-spin S (a good quantum number) can be expanded in terms of a few basis-states $f_{S,i}$. Let $P^{\lambda}_{f_{S,i}}$ be the probability of a pair of spins coupled to $\lambda = 0, 2, 4$, and 6 in the $f_{S,i}$ state. Obviously, when the strength g_λ of the λ-channel is more negative, the basis-state with the largest $P^{\lambda}_{f_{S,i}}$ would be more preferred by the g.s.. When two strengths are more negative, the two basis-states with the two largest probabilities would be more important components. Thus, based on the probabilities, the spin-structures (described via the basis-states) can be understood. Furthermore, all the details in the phase-diagrams, say, the critical points of transition, can also be explained. Note that, for $f_{S,i}$, $P^{\lambda}_{f_{S,i}}$ is completely determined by symmetry. Thus, symmetry plays a very important role in determining the spin-structure of the g.s..

It is recalled that, due to the realization of optical trapping about 20 years ago, the field of Bose–Einstein condensates has been greatly extended and the spin-degrees of freedom begin to play their roles. On the other hand, a notable progress in recent years is the technique in the trapping and manipulation of a few cold atoms (molecules)[1]. This technique could also extend the field greatly from traditional many-body systems to cold few-body systems. In the theoretical aspect, the former can only be solved approximately, while the latter can be solved exactly and detailed analysis on the spin-structures can be made. Thus the knowledge extracted from few-body systems would be a complement to those from many-body systems. Furthermore, for cold atoms, the temperature can be tuned so low (say, $T < 10^{-10}$ K) that the spatial degrees of freedom are nearly frozen. This leads to a kind of cold few-body systems having only spin-degrees of freedom. Note that all few-body systems are strongly constrained by symmetry so that the quantum states are governed by a few quantum numbers. Obviously, due to the difference in degrees of freedom, the effects of symmetry constraint imposing on usual and cold few-body systems are different (as shown in a previous paper[2]). Thus, the field of the study of few-body systems could also be thereby extended and rich physics would be involved. Therefore, the study of cold few-body systems, they are scarcely studied before, is meaningful.

For many-body systems, there are a number of literatures dedicated to the study of spin-1[3–11] and spin-2 cold atoms[10,12–19]. Those for spin-3 condensates are fewer, where the spin-structures appear to be complicated[20–26]. This paper, as a continuation of[2], is dedicated to four-body systems with spin-3 cold atoms. The purpose is to find out the spin-structures of the ground states (g.s.). Note that the interaction contains four parameters $\{g_\lambda\}$ (where λ is the coupled spin of two atoms). A negative g_λ would push a pair of atoms to form a $[\lambda]$-pair ($\lambda = 0$, 2, 4, and 6). We believe that, when g_λ is sufficiently negative, the $[\lambda]$-pairs would be important constituents. When two or more g_λ are negative, there is competition among them. We will see how the competition would be under the constraint from symmetry.

Spin-dependent Hamiltonian and the eigen-states

Let N spin-3 atoms (say, Cr, Mo, Sn, Pu) be confined in an optical trap. It is assumed that the temperature is so low and the binding is so strong that all the particles have condensed to a spatial state $\phi(\mathbf{r})$ which is most favorable for binding. While all the spatial degrees of freedom are frozen, the spin-degrees of freedom remain free, therefore various spin-structures can be formed. These structures depend essentially on the spin-dependent Hamiltonian, which can be written as

[1]Department of physics, Shaoguan University, Shaoguan 510205, People's Republic of China. [2]School of Physics, Sun Yat-Sen University, Guangzhou 510275, People's Republic of China. ✉email: stsbcg@mail.sysu.edu.cn

$$H_{spin} = \sum_{i<j} V_{ij},$$
$$V_{ij} = \sum_{\lambda} g_\lambda P_\lambda^{ij},$$

where i (j) denotes a particle. $\lambda = 0, 2, 4$, and 6 is the coupled spin of a pair, P_λ^{ij} is the projector to the λ -channel. g_λ is the weighted strength which is a product of the strength and the integral $\int \phi^4 d\mathbf{r}$. The latter embodies the effect of spatial profile. The dipole–dipole (d–d) coupling between a pair of atoms is relatively weak (for ^{52}Cr as an example, the strength of the d–d coupling $c_{dd} = 0.004 g_6$), therefore is neglected. In fact, the calculation in[21] demonstrates that the g.s. of ^{52}Cr does not seem to depend on the d–d coupling. An important feature of H_{spin} is the conservation of the total spin S and its Z-component M . Thus the eigen-energies and eigen-states of H_{spin} are denoted as E_{SM} and ψ_{SM} (the subscript M might be neglected).

We introduce the Fock-states $|\alpha\rangle \equiv |N_{3\alpha}, N_{2\alpha}, \ldots N_{-3,\alpha}\rangle$, where α represents a set of seven numbers $\{N_{\mu\alpha}\}$ $(-3 \le \mu \le 3)$, $N_{\mu\alpha}$ is the number of particles in μ magnetic component. Obviously, $\Sigma_\mu N_{\mu\alpha} = N$ and $\Sigma_\mu \mu N_{\mu\alpha} = M$. The Fock-states are adopted as basis-states for diagonalizing H_{spin}. The matrix element is

$$\begin{aligned}\langle\alpha'|H_{spin}|\alpha\rangle =& \frac{1}{2}\sum_{\mu'\nu'\mu\nu}\delta_{\mu'+\nu',\mu+\nu}\sum_\lambda g_\lambda C^{\lambda,\mu'+\nu'}_{3\mu';3\nu'} C^{\lambda,\mu+\nu}_{3\mu;3\nu} \\ &\cdot\Big(\bar\delta_{\mu'\nu'}\bar\delta_{\mu\nu}\sqrt{N'_{\mu'}N'_{\nu'}N_\mu N_\nu}\,\delta_{[\alpha']_{\mu'\nu'};[\alpha]_{\mu\nu}} \\ &+\bar\delta_{\mu'\nu'}\delta_{\mu\nu}\sqrt{N'_{\mu'}N'_{\nu'}N_\mu(N_\mu-1)}\,\delta_{[\alpha']_{\mu'\nu'};[\alpha]_{\mu\mu}} \\ &+\delta_{\mu'\nu'}\bar\delta_{\mu\nu}\sqrt{N'_{\mu'}(N'_{\mu'}-1)N_\mu N_\nu}\,\delta_{[\alpha']_{\mu'\mu'};[\alpha]_{\mu\nu}} \\ &+\delta_{\mu'\nu'}\delta_{\mu\nu}\sqrt{N'_{\mu'}(N'_{\mu'}-1)N_\mu(N_\mu-1)}\,\delta_{[\alpha']_{\mu'\mu'};[\alpha]_{\mu\mu}}\Big)\end{aligned}$$

where $|\alpha'\rangle \equiv |N'_{3\alpha}, \cdots\rangle$, $\delta_{\mu\nu} = 1$ or 0 (if $\mu = \nu$ or $\neq \nu$), $\bar\delta_{\mu\nu} = 1 - \delta_{\mu\nu}$, $\delta_{[\beta];[\alpha]} = 1$ (if all the seven numbers in $[\beta]$ are one-to-one identical to those in $[\alpha]$) or 0 (otherwise), the Clebsch–Gordan coefficients have been introduced. Carrying out the diagonalization, E_{SM} together with

$$\psi_{SM} = \sum_\alpha D^S_\alpha |\alpha\rangle$$

can be obtained. The total number of Fock-states is bound by N and M. Since no magnetic field is applied, S of an eigen-state can be known by its degeneracy. In particular, the lowest eigen-state (g.s.) is denoted as $\Psi_{S(gs)}$ which we will focus on.

Spin-structures based on the pairs

After the diagonalization of H_{spin}, the parameter space can be divided into zones according to S, and the phase diagram thereby can be plotted. To reduce the complexity, we use three 2-dimensional subspaces to replace the 4-dimensional parameter space as shown in Fig. 1. In each of these subspaces g_4 and g_6 are variable, while g_0 and g_2 are fixed. There are three possible cases (1) $g_0 < g_2$, (2) $g_0 \simeq g_2$, and (3) $g_0 > g_2$. Note that the spin-structures will neither be changed when all the $\{g_\lambda\}$ are shifted with the same value, nor when the unit for $\{g_\lambda\}$ is changed. For case (1), let the set $\{g_\lambda\}$ be shifted so that $(g_0 + g_2)/2 = 0$, then a unit is adopted so that $g_0 = -0.5$ and $g_2 = 0.5$ (Fig. 1a). For case (2), as an approximation, we assume $g_0 = g_2$. Then, $\{g_\lambda\}$ is shifted so that $g_0 = g_2 = 0$ (Fig. 1b). For case (3), similarly, we have $g_0 = 0.5$ and $g_2 = -0.5$ (Fig. 1c). For all the three cases, the ranges of g_4 and g_6 are from -1 to $+1$. In the qualitative sense, the feature of a 4-dimensional diagram can be roughly illustrated via these three 2-dimensional diagrams.

To understand better the underlying physics, in addition to numerical solutions, we look for analytical solutions. Let

$$\tilde{\varphi}_{(\lambda_a\lambda_b)_S} = \mathfrak{S}[(\chi(1)\chi(2))_{\lambda_a}(\chi(3)\chi(4))_{\lambda_b}]_S \equiv \mathfrak{S}\varphi_{S;\lambda_a\lambda_b}$$

be a basis-state,where $\mathfrak{S}$ is an operator for symmetrization and normalization, $\chi(i)$ is the spin-state of the i-th particle, particles 1 and 2 (3 and 4) are coupled to λ_a (λ_b), λ_a and λ_b should be even and coupled to S. Note that$\varphi_{S;\lambda_a\lambda_b}$ has not yet been symmetrized, but $\tilde{\varphi}_{(\lambda_a\lambda_b)_S}$ is. When S is fixed while λ_a and λ_b are variable, the set $\{\tilde{\varphi}_{(\lambda_a\lambda_b)_S}\}$ can also be used as (non-orthogonal) basis-states for ψ_{SM}. It turns out that, for N = 4, the multiplicity of every ψ_{SM} is very small (≤ 3). Thus H_{spin} can be analytically diagonalized. Examples are given below.

By recoupling the spins, we have

$$\tilde{\varphi}_{(\lambda_a\lambda_b)_S} = \Sigma_{\lambda'_a\lambda'_b} C_{S;\lambda_a\lambda_b;\lambda'_a\lambda'_b}\varphi_{S;\lambda'_a\lambda'_b}$$

where

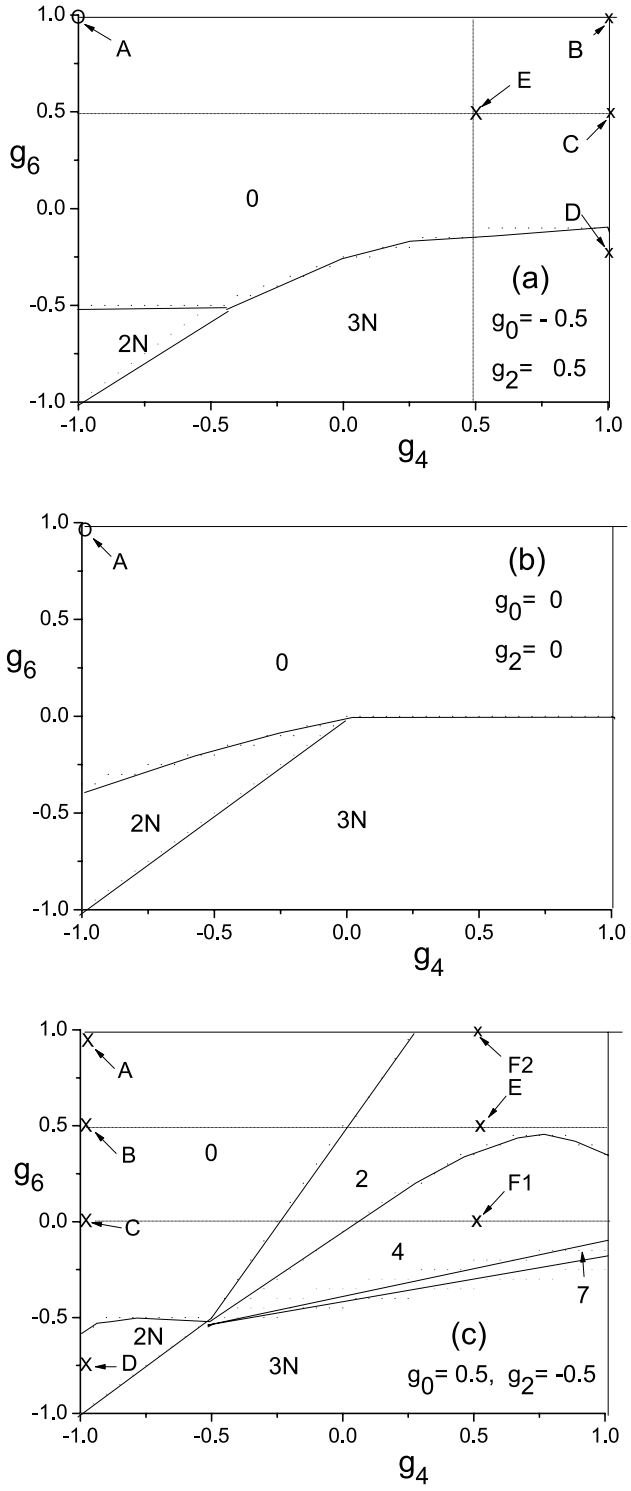

Figure 1. Phase diagrams of the g.s. of N = 4 systems against g_4 and g_6, while g_0 and g_2 are fixed and marked in the panels. S is marked on the associated zone.

$$C_{S;\lambda_a\lambda_b;\lambda'_a\lambda'_b} = \gamma\left(\delta_{\lambda_a\lambda'_a}\delta_{\lambda_b\lambda'_b} + (-1)^S\delta_{\lambda_a\lambda'_b}\delta_{\lambda_b\lambda'_a} + 4\overline{\lambda_a}\overline{\lambda_b}\overline{\lambda'_a}\overline{\lambda'_b}\begin{Bmatrix} 3 & 3 & \lambda_a \\ 3 & 3 & \lambda_b \\ \lambda'_a & \lambda'_b & S \end{Bmatrix}\right)$$

where γ is a coefficient for normalization, the quantity with {} is a 9-j symbol, and $\overline{\lambda_a} \equiv \sqrt{2\lambda_a + 1}$, etc.

λ	0	2	4	6
$C_{0;00;\lambda\lambda}$	0.6547	0.3253	0.4364	0.5245
$C_{0;22;\lambda\lambda}$	0.3061	0.6958	−0.4591	0.4598
$C_{0;44;\lambda\lambda}$	0.3292	−0.3681	0.8679	0.0540
$C_{0;66;\lambda\lambda}$	0.5941	0.5535	0.0810	0.5780

Table 1. The coefficients in the expansion of ψ_{SM} when $S = 0$

The multiplicity of $S = 0$ states is two. Therefore, among the four basis-states $\{\tilde{\varphi}_{(\lambda,\lambda)_0}\}$, it is sufficient to choose $\tilde{\varphi}_{(4,4)_0}$ and $\tilde{\varphi}_{(6,6)_0}$ for the expansion of ψ_{SM}. Other $\tilde{\varphi}_{(\lambda,\lambda)_0}$ state is simply a linear combination of them. Note that these two basis-states are not exactly orthogonal to each other. Instead, $\langle\tilde{\varphi}_{(4,4)_0}|\tilde{\varphi}_{(6,6)_0}\rangle \equiv O_{4,6} = \Sigma_\lambda C_{0;44;\lambda\lambda}C_{0;66;\lambda\lambda} = 0.0933$, where $C_{0;\lambda\lambda;\lambda'\lambda'}$ is given in the table.For $S = 0$ states, the associated matrix elements are

$$H_{4,4} \equiv \langle\tilde{\varphi}_{(4,4)_0}|H_{spin}|\tilde{\varphi}_{(4,4)_0}\rangle = 6\Sigma_\lambda C^2_{0:44;\lambda\lambda}g_\lambda,$$

$$H_{6,6} \equiv \langle\tilde{\varphi}_{(6,6)_0}|H_{spin}|\tilde{\varphi}_{(6,6)_0}\rangle = 6\Sigma_\lambda C^2_{0;66;\lambda\lambda}g_\lambda,$$

$$H_{4,6} = H_{6,4} \equiv \langle\tilde{\varphi}_{(4,4)_0}|H_{spin}|\tilde{\varphi}_{(6,6)_0}\rangle = 6\Sigma_\lambda C_{0;44;\lambda\lambda}C_{0;66;\lambda\lambda}g_\lambda$$

where the set $\{C_{0;\lambda'\lambda';\lambda\lambda}\}$ are listed in the table:

The eigen-energy E_0 is the root of a two-dimensional homogeneous linear equation,

$$\left(E_0 - H_{4,4}\right)\left(E_0 - H_{6,6}\right) - \left(E_0O_{4,6} - H_{4,6}\right)\left(E_0O_{4,6} - H_{4,6}\right) = 0$$

Making use of Table 1, the eigen-energy of the lower $S = 0$ states is

$$E_{0(-)} = \frac{6}{1.9826}\left(B - \sqrt{B^2 - 3.9652D}\right)$$

where

$$B = 0.4248g_0 + 0.4799g_2 + 0.7467g_4 + 0.3312g_6$$

$$D = 0.1607g_0g_2 + 0.2391g_0g_4 + 0.0250g_0g_6 \ + 0.2603g_2g_4 + 0.0589g_2g_6 + 0.2473g_4g_6$$

The normalized spin-state of the lower $S = 0$ state is

$$\psi_{0(-)} = a_4\tilde{\varphi}_{(4,4)_0} + a_6\tilde{\varphi}_{(6,6)_0}$$

where

$a_4 = 1/\sqrt{1 + x^2 + 2xO_{4,6}}$, $x = (H_{4,4} - E_{0(-)})/(O_{4,6}E_{0(-)} - H_{4,6})$, and $a_6 = xa_4$.

The weight of $\tilde{\varphi}_{(4,4)_0}$ in $\psi_{0(-)}$ is $\langle\tilde{\varphi}_{(4,4)_0}|\psi_{0(-)}\rangle^2 = (a_4 + a_6O_{4,6})^2$. Similarly, the weight of $\tilde{\varphi}_{(6,6)_0}$ is equal to $(a_6 + a_4O_{4,6})^2$. If other $\tilde{\varphi}_{(\lambda\lambda)_0}$ are chosen to replace $\tilde{\varphi}_{(4,4)_0}$ and/or $\tilde{\varphi}_{(6,6)_0}$, the resultant $E_{0(-)}$ and $\psi_{0(-)}$ are not changed.

For $S = 2$ and 8 (both have multiplicity two), $E_{S(-)}$ and $\psi_{S(-)}$ can be similarly obtained. For $S = 4$ and 6 (both have multiplicity three), the analytical solutions are more complicated.

Whereas for $S = 3$, 5, 7, 9, 10 and 12 states, all of them have multiplicity one, thus the eigen-state is just $\tilde{\varphi}_{(\lambda_a\lambda_b)_S}$, where λ_a and λ_b are arbitrary even numbers adapted to S. For example, when $S = 7$ we choose $\lambda_a = 6$ and $\lambda_b = 4$, then we have

$$\psi_{7M} = \tilde{\varphi}_{(6,4)_7} = \Sigma_{\lambda'_a\lambda'_b}C_{7;6,4;\lambda'_a\lambda'_b}[(\chi(1)\chi(2))_{\lambda'_a}(\chi(3)\chi(4))_{\lambda'_b}]_7$$

where $C_{7;6,4;2,6} = .6362$, $C_{7;6,4;4,6} = .3086$, $C_{7;6,4;6,2} = -C_{7;6,4;2,6}$, $C_{7;6,4;6,4} = -C_{7;6,4;4,6}$, otherwise $C_{7;6,4;\lambda'_a\lambda'_b} = 0$. The eigen-energy

$$E_{S=7} = 6\left[C^2_{7;6,4;2,6}g_2 + C^2_{7;6,4;4,6}g_4 + \left(C^2_{7;6,4;2,6} + C^2_{7;6,4;4,6}\right)g_6\right]$$

The eigen-energies of other S-states with multiplicity can be similarly obtained.It is emphasized that, when other λ_a and λ_b are chosen, both ψ_{7M} and $E_{S=7}$ remain the same. These states are strictly determined by symmetry.

In particular, when $S = 3N$, we have $E_{S=3N} = \frac{N(N-1)}{2} g_6$. With the help of the analytical solutions, the physics inherent in Fig. 1 can be better understood, we found

(1) When $g_4 < 0$ and $g_6 > 0$ (up-left quadrant in Fig. 1) only $S = 0$ state is found.
Note that, when a g_λ is more negative than the others, two spins in the g.s. will prefer to be coupled to λ and form a $[\lambda]$-pair. Let $\langle(\lambda_a\lambda_b)_S|gs\rangle$ be a shortened label for the overlap $\langle\tilde{\varphi}_{(\lambda_a\lambda_b)_S}|\Psi_{S(gs)}\rangle$. We found that, at the point A (where $g_4 = -1$ and $g_6 = 1$) marked in Fig. 1a–c, $\langle(4,4)_0|gs\rangle = 0.9883$, 0.9996, and 0.9794, respectively. It implies that the g.s. is essentially composed of two [4]-pairs (due to the very negative g_4), and they are further coupled to zero, namely, they are lying opposite to each other (due to the very positive g_6). Besides, at C, B and A marked in Fig.1c (where $g_6 = 0$, 0.5, and 1), $\langle(4,4)_0|gs\rangle$ =0.9703, 0.9765, and 0.9883, respectively. It implies that, when g_6 increases from 0, the structure $(4,4)_0$ will be more dominant.

(2) When g_4 and g_6 are both negative (down-left quadrant), $S = 0$, 8, and 12 states are found.
For Fig. 1c as an example, when $g_4 = -1$ and $g_6 = 0$ (point C), -0.75 (point D), and -1.1, we found $\langle(4,4)_0|gs\rangle$ =0.9703, $\langle(4,4)_8|gs\rangle = 0.966$, and $\langle(6,6)_{12}|gs\rangle = 1$, respectively. Thus S undergoes a transition as 0→8→12. It implies that the decrease of g_6 causes first a change of the relative orientation of the two [4]-pairs (from being anti-parallel to parallel), then a succeeded breakdown of the [4]-pairs and leading to a full polarization. The transition of S takes place when either $E_{0(gs)} = E_{8(gs)}$ or $E_{8(gs)} = E_{12(gs)}$. Since the analytical expressions of the energies have been given, the critical points of transition can be analytically obtained.

(3) In up-right quadrant with $g_4 > 0$ and $g_6 > 0$, if $g_0 \leq 0$ (Fig. 1a,b), we found the [0]-pairs. For example,s at the point B, C and E in Fig. 1a, we have $\langle(0,0)_0|gs\rangle = 0.982$, 0.970, and 0.993, respectively. Whereas if $g_2 \leq 0$ (1c) we found the [2]-pairs. For examples, at the point F2, E and F1, we have $\langle(2,2)_2|gs\rangle = 1.000$, $\langle(2,2)_2|gs\rangle = 0.993$, and $\langle(2,2)_4|gs\rangle = 0.974$, respectively. In these examples we see once more how the relative orientation of the two $[\lambda]$-pairs is adjusted by g_6.

(4) When $g_4 > 0$ and $g_6 < 0$ (down-right quadrant), the g.s. mostly has $S = 12$ and the g.s. is fully polarized.

(5) Making use of the analytical solutions, all the boundaries in the phase diagrams can be analytically described via the equation $E_{S(gs)} = E_{S'(gs)}$. For an example, in Fig. 1c, the boundary separating the zones with $S = 12$ and $S' = 7$ satisfies $g_6 = 0.1904, g_4 = 0.4048$. This explains why this boundary is a straight line up-rising slowly with g_4.

Competition in the formation of pairs

From the above section we know that, when a g_λ is more negative than the others, the $[\lambda]$-pairs will be important. The relative orientation of the spins of pairs depends on g_6 and will be changed from being anti-parallel to parallel. It is expected that, when g_λ and $g_{\lambda'}$ are both more negative, there would be a competition between the $[\lambda]$- and $[\lambda']$-pairs. To clarify, we introduce another kind of phase diagrams as shown in Fig. 2.

In Fig. 2a both g_4 and g_2 are negative, thus there is a competition between the [4]- and [2]-pairs

When $g_6 = -1$ (horizontal black line), due to the strong attraction caused by g_6, no $[\lambda]$-pairs ($\lambda \neq 6$) would emerge. Instead, all the spins are aligned and the g.s. is fully polarized.

When $g_6 = -0.5$ (dash), both [4]-, [2]-, and [6]-pairs might emerge. When $g_4 < g_2$, the g.s. is dominated by $(4,4)_8$ (say, when $g_4 = -0.75$, $\langle(4,4)_8|gs\rangle_{g_4=-0.75} = 0.966$). There is a critical point $p_{8\to4}$ located at $g_4 = g_2 = -0.5$, at which S transits from 8 to 4. Afterward, when g_4 (g_2) increases (decreases) further so that $g_2 < g_4$, the g.s. is dominated by $(2,2)_4$ (say, $\langle(2,2)_4|gs\rangle_{g_4=-0.25} = 0.967$). Thus the negative $g_6 = -0.5$ is not sufficient to form the [6]-pairs, but sufficient to bring the spins of the two [4]-pairs or the two [2]-pairs to be parallel.

When $g_6 = 0$ (dash–dot). Due to the vanish of the attraction from g_6, the two [4]- or [2]-pairs are no more parallel. There is a critical point $p_{0\to2}$ (where $g_4 = -0.333$) and a point of balance B_1 (where $g_4 = -0.391$). When $g_4 < p_{0\to2}$, the g.s. is composed of $(4,4)_0$ and $(2,2)_0$. The pair $(4,4)_0$ would be more important if $g_4 < B_1$, whereas $(2,2)_0$ would be if $g_4 > B_1$, and they would arrive at a balance at B_1, i.e., $\langle(4,4)_0|gs\rangle_{g_4=-0.391} = \langle(2,2)_0|gs\rangle_{g_4=-0.391} = 0.874$ (note: $\langle(4,4)_0|(2,2)_0\rangle \neq 0$). The point $p_{0\to2}$ marks the transition of S from 0 to 2. When $g_4 > p_{0-2}$, the g.s. is essentially $(2,2)_2$ (say, $\langle(2,2)_2|gs\rangle_{g_4=-0.32} = 0.986$, $\langle(2,2)_2|gs\rangle_{g_4=-0.1} = 1.000$).

The case with $g_6 = 0.5$ (solid line in orange) is similar to the case with $g_6 = 0$, except $p_{0\to2} = -0.163$, and the balance point $B_2 = -0.274$. Thus, both $p_{0\to2}$ and B_2 shift to the right.

When $g_6 = 1$ (dot), the case is also similar to the above case, however the critical point shifts to the right and beyond the range $-1 < g_4 \leq 0$ (therefore it can not be seen). The repulsion caused by g_6 is sufficiently strong so that the pairs kept to be anti-parallel, and therefore the g.s. is composed of $(4,4)_0$ and $(2,2)_0$ with the balance point B_3 at $g_4 = -0.157$. Say, $\langle(4,4)_0|gs\rangle_{g_4=-1} = 1.000$, $\langle(4,4)_0|gs\rangle_{g_4=-0.157} = \langle(2,2)_0|gs\rangle_{g_4=-0.157} = 0.874$, and $\langle(2,2)_0|gs\rangle_{g_4=0} = 0.942$.

We found $B_1 < B_2 < B_3$. Note that, when g_6 is positive, the formation of [6]-pairs is unfavorable to the energy. Let the probability of two spins coupled to λ in a state Φ be P^λ_Φ. Then, $P^6_{(\lambda\lambda)_0} = (C_{0;\lambda\lambda;6,6})^2 = (0.4598)^2$ (if $\lambda = 2$) and $= (0.0540)^2$ (if $\lambda = 4$). Thus the appearance of the [6]-pairs in $(4,4)_0$ is much less probable than in $(2,2)_0$. Therefore, the structure $(4,4)_0$ would be more favorable than $(2,2)_0$ when g_6 becomes more positive. This explains the reason that the balance point shifts to the right.

Furthermore, when g_6 increases, the critical point also shifts to the right. This is due to a similar reason that the appearance of the [6]-pairs in $(2,2)_0$ is less probable than in $(2,2)_2$.

In Fig. 2b both g_0 and g_4 are negative.

Figure 2b is comparable with Fig. 2a, but the following distinctions are noticeable.

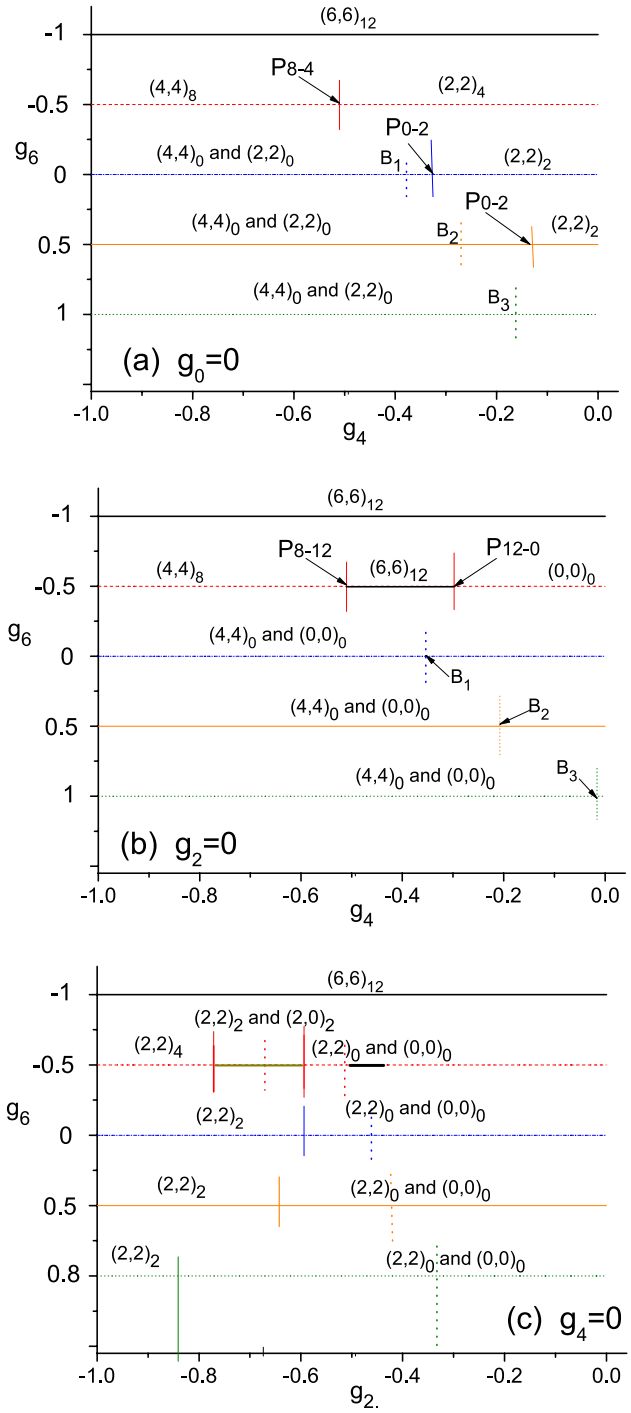

Figure 2. The dominant component(s) in the spin-structure of the g.s. The label of the component $(\lambda_a, \lambda_b)_S$ is marked above the horizontal lines, each is for a given g_6 marked at the left end of the line. For 2a, $g_0 = 0$, the abscissa is for g_4, and $g_2 = -1 - g_4$. For 2b, $g_2 = 0$, the abscissa is also for g_4, and $g_0 = -1 - g_4$. For 2c, $g_4 = 0$, the abscissa is for g_2, and $g_0 = -1 - g_2$.

(1) In this case the [0]-pairs and [4]-pairs are competing. Accordingly, when $g_6 \geq 0$, the two important and competing component are $(4,4)_0$ and $(0,0)_0$ (rather than $(2,2)_0$).
(2) When $g_6 \geq 0$, g_0 and g_4 are both negative. Thus, both the [4]-pair and [2]-pair are important and they are competing. Meanwhile, g_6 is sufficiently positive to keep the two [λ]-pairs anti-parallel so that S is kept to be zero and the transition of S from 0 to 2 does not appear.
(3) When g_6 becomes negative, there is competition among the [6], [4], and [0]-pairs. Say, when $g_6 = -0.5$ and $-0.51 < g_4 < -0.29$, the [6]-pairs emerge in the middle segment of the dash-line. They will be changed to the [4]-pairs if g_4 becomes more negative, or to the [0]-pairs if g_0 becomes more negative. For the dash-line,

due to the negative g_6, either the two [4]-pairs or the two [6]-pairs are parallel to each other. This leads to the transition of S as $8 \rightarrow 12 \rightarrow 0$ when g_4 increases (g_0 decreases).

(4) The shift of the balance point to the right appears again (i.e., $B_1 < B_2 < B_3$). Note that $C_{0;0,0;6,6} = 0.5245$. Thus the appearance of the [6]-pairs in $(4,4)_0$ is also much less probable than in $(0,0)_0$. This causes the shift as before.

In Fig. 2c both g_0 and g_2 are negative.

When $g_6 = -1$, the g.s. is fully polarized as before. Otherwise, the g.s. is essentially composed of $(2,2)_{\lambda_b}$ and $(0,0)_0$ (where $\lambda_b = 4$, 2, and 0). When $g_6 = -0.5$ we see a chain of transitions: S=4 $\rightarrow$ 2 $\rightarrow$ 0 $\rightarrow$ 12 $\rightarrow$ 0.When g_0, g_2 and g_6 are all close to -0.5, there is a small segment in bold black line where $(6,6)_{12}$ emerges (similar to the case in Fig. 2b). When $g_6 = 0$, 0.5, and 0.8 (dotted line), we see the transition of $S = 2 \rightarrow 0$. Where the critical point shifts to the left when g_6 increases. It implies that the appearance of the [6]-pairs in $(2,2)_0$ is less probable than in $(2,2)_2$. Whereas the balance point shifts to the right when g_6 increases. It implies that the appearance of the [6]-pairs in $(2,2)_0$ is less probable than in $(0,0)_0$.

Final remarks

The spin-structures of $N = 4$ condensates have been studied, both numerical and analytical solutions have been obtained. Thereby two kinds of phase-diagrams for the g.s. have been plotted and explained. From dynamical aspect, the $[\lambda]$-pairs would be important constituents when g_λ is more negative. However, the probability of the appearance of a $[\lambda]$-pair in a particular component $(\lambda_a\lambda_b)_S$ is determined by symmetry. Thus the structure of the g.s. depends not only on the strengths but also on the symmetry constraint. We have calculated the probabilities $P^{\lambda}_{(\lambda_a\lambda_b)_S}$ for finding out the important components. The importance is further confirmed by the calculation of the amplitudes $\langle(\lambda_a\lambda_b)_S|\Psi_{S(gs)}\rangle$. Obviously, for cold few-body systems, the very small multiplicity of a state is a remarkable feature, thereby the states are tightly (or even completely) constrained by symmetry.

When two or more g_λ are negative and close to each other, there is competition between various $[\lambda]$-pairs and the most important pair is thereby determined. Note that the magnitude of S depends on the relative orientation of the pair-spins λ_a and λ_b (if they are nonzero), while the orientation is determined by the strengths. In particular, the sign of g_6 is crucial which determines whether the two pair-spins are parallel or anti-parallel. Thus the variation of $\{g_\lambda\}$ will cause the change of the most important pair and the relative orientation of the pair-spins. This leads to the shift of the balance point and the critical point. The chain of transitions is thereby explained.

The approach of this paper can be generalized to systems with a larger N. When N is larger, if g_λ is more negative, the $[\lambda]$-pairs would also be more important in the g.s. There would also be competitions among various $[\lambda]$-pairs. The study of the probability P^{λ}_{Φ} where Φ is an assumed basis-state would also be helpful for finding out the important component(s) and their alternation. In particular, some very stable spin-structures found in few-body systems could be building blocks for large N systems. This is a point to be clarified.

Received: 6 March 2021; Accepted: 26 August 2021
Published online: 09 September 2021

References

1. Meyer, G. *et al.* Controlled manipulation of atoms and small molecules with a low temperature scanning tunneling microscope. *Single Molecules* **1**(1), 79 (2000).
2. Liu, Y. M., He, Y. Z. & Bao, C. G. A stable spin-structure found in a 3-body system with spin-3 cold atoms and its role in N-body condensates. *Sci. Rep.* **11**, 1792 (2021).
3. Stenger, J. *et al.* Spin domains in ground-state Bose–Einstein condensates. *Nature* **396**, 345 (1998).
4. Stamper-Kurn, D. M. *et al.* Optical confinement of a Bose–Einstein condensate. *Phys. Rev. Lett.* **80**, 2027 (1998).
5. Ho, T. L. Spinor Bose condensates in optical traps. *Phys. Rev. Lett.* **81**, 742 (1998).
6. Ohmi, T. & Machida, K. Bose–Einstein condensation with internal degrees of freedom in alkali atom gases. *J. Phys. Soc. Jpn.* **67**, 1822 (1998).
7. Law, C. K., Pu, H. & Bigelow, N. P. Quantum spins mixing in spinor Bose–Einstein condensates. *Phys. Rev. Lett.* **81**, 5257 (1998).
8. Goldstein, E. V. & Meystre, P. Quantum theory of atomic four-wave mixing in Bose–Einstein condensates. *Phys. Rev. A* **59**, 3896 (1999).
9. Ho, T. L. & Yip, S. K. Fragmented and single condensate ground states of spin-1 bose gas. *Phys. Rev. Lett.* **84**, 4031 (2000).
10. Koashi, M. & Ueda, M. Exact Eigenstates and magnetic response of spin-1 and spin-2 Bose–Einstein condensates. *Phys. Rev. Lett.* **84**, 1066 (2000).
11. Li, Z. B., Yao, D. X. & Bao, C. G. Spin-thermodynamics of ultra-cold spin-1 atoms. *J. Low Temp. Phys.* **180**, 200 (2015).
12. Ciobanu, C. V., Yip, S. K. & Ho, T. L. Phase diagrams of F = 2 spinor Bose–Einstein condensates. *Phys. Rev. A* **61**, 033607 (2000).
13. Ueda, M. & Koashi, M. Theory of spin-2 Bose–Einstein condensates: Spin correlations, magnetic response, and excitation spectra. *Phys. Rev. A* **65**, 063602 (2002).
14. Van, Isacker P. & Heinze, S. Bose–Einstein condensates of atoms with arbitrary spin. *J. Phys. A Math. Theor.* **40**, 14811 (2007).
15. Chacon, E., Moshinsky, M. & Sharp, R. T. U(5)⊆O(5)⊆O(3) and the exact solution for the problem of quadrupole vibrations of the nucleus. *J. Math. Phys.* **17**, 668 (1976).
16. Gheorghe, A. & Raduta, A. A. New results for the missing quantum numbers labelling the quadrupole and octupole boson basis. *J. Phys. A Math. Gen.* **37**, 10951 (2004).
17. Kawaguchi, Y. & Ueda, M. Spinor Bose–Einstein condensates. *Phys. Rep.* **520**, 253 (2012).
18. Stamper-Kurn, D. M. & Ueda, M. Spinor Bose gases: Symmetries, magnetism, and quantum dynamics. *Rev. Mod. Phys.* **85**, 1191 (2013).
19. He, Y. Z., Liu, Y. M. & Bao, C. G. Generalized Gross–Pitaevskii equation adapted to the U(5)⊃SO(5)⊃ SO(3)symmetry for spin-2 condensates. *Phys. Rev. A* **91**, 033620 (2015).
20. Santos, L. & Pfau, T. Spin-3 chromium Bose–Einstein condensates. *Phys. Rev. Lett.* **96**, 190404 (2006).
21. Makela, H. & Suominen, K.-A. Ground states of spin-3 Bose–Einstein condensates for conserved magnetization. *Phys. Rev. A* **75**, 033610 (2007).
22. Uchino, S., Otsuka, T. & Ueda, M. Dynamical symmetry in spinor Bose–Einstein condensates. *Phys. Rev. A* **78**, 023609 (2008).

23. Huhtamaki, J. A. M. *et al.* Spin textures in condensates with large dipole moments. *Phys. Rev. A* **81**, 063623 (2010).
24. Pasquiou, B. *et al.* Thermodynamics of a Bose–Einstein condensate with free magnetization. *Phys. Rev. Lett.* **108**, 045307 (2012).
25. Situ, S. P. & He, Y. Z. The spin evolution of spin-3 ^{52} Cr Bose–Einstein condensate. *Chin. Phys. B* **20**, 010310 (2011).
26. He, Y. Z., Chen, Z. F., Li, Z. B. & Bao, C. G. Evaluation of the 52Cr–52Cr interaction via spin–flip scattering. *Few-Body Syst.* **46**, 257 (2009).

Acknowledgements

Supported by the National Natural Science Foundation of China under Grants nos. 11372122 and 10874122; Key Scientific Research Platforms and Projects of Ordinary Universities of Guangdong of China (2020KCXTD024).

Author contributions

Y.M.L. is for theoretical derivation and numerical calculation, C.G.B. propose the idea and write the paper.

Declarations

Competing interests

The authors declare no competing interests.

Additional information

Correspondence and requests for materials should be addressed to C.G.B.

Reprints and permissions information is available at www.nature.com/reprints.

Publisher's note Springer Nature remains neutral with regard to jurisdictional claims in published maps and institutional affiliations.

Open Access This article is licensed under a Creative Commons Attribution 4.0 International License, which permits use, sharing, adaptation, distribution and reproduction in any medium or format, as long as you give appropriate credit to the original author(s) and the source, provide a link to the Creative Commons licence, and indicate if changes were made. The images or other third party material in this article are included in the article's Creative Commons licence, unless indicated otherwise in a credit line to the material. If material is not included in the article's Creative Commons licence and your intended use is not permitted by statutory regulation or exceeds the permitted use, you will need to obtain permission directly from the copyright holder. To view a copy of this licence, visit http://creativecommons.org/licenses/by/4.0/.

© The Author(s) 2021